Superlinear Angular Momentum in Reaction Wheels

Seth Hinz

April 19, 2021

1 Introduction

In several robotics applications, reaction wheels are used to control the rotation of a body. However, they do have some drawbacks - size, mass, and controllability are all important factors to consider. For my term project, I will be analyzing a reaction wheel with variable radius, which may offer mitigations to these shortcomings.

2 Background

Before we introduce a reaction wheel with variable radius, it is useful to examine the simpler fixed-radius case. To provide the largest moment of inertia, we will model the reaction wheel as a thin ring of mass m at a radius r from the axis of rotation (which, importantly, is the symmetry axis of the ring).

TODO IMAGE HERE

From this model, we can calculate the moment of inertia via integrating over the mass:

$$
\begin{align}
I &= \oint_{\text{ring}} \mathrm{d}m \tag{1}\\
&= \int_0^{2\pi} (\frac{m}{2\pi r})(r^2) r \mathrm{d}\theta \tag{2}\\
&= \frac{mr^2}{2\pi} \int_0^{2\pi} \mathrm{d}\theta \tag{3}\\
&= mr^2 \tag{4}
\end{align}
$$

Using this result, we can now find the angular momentum of the system.

$$
\begin{align}
L &= I\omega \tag{5}\\
&= \omega m r^2 \tag{6}
\end{align}
$$

Earlier, I stated that the controllability of a reaction wheel needs to be considered during the design process. Equation (6) shows why this is true - the angular momentum added to a body by a reaction wheel is only linear in the angular velocity. So, if a large amount of angular acceleration is needed quickly, a motor driving a reaction wheel must drastically alter its speed.

3 Variable Radius

The motivation for using a wheel with changing radius can now be illustrated. If the radial term in equation (6) was replaced by an increasing function in ω (namely, $L(\omega) = m\omega \cdot r(\omega)^2$), then we could push $L(\omega)$ far above linearity. Any motor speed decrease that maintains angular momentum will come at the cost of a larger torque, of course, but this may be a desirable tradeoff.

This insight led me to investigate a reaction wheel that uses discrete, spring-affixed masses about a central hub. In this model, each spring is flexible in only the radial direction, which reduces the number of degrees of freedom in this problem. Each appendage has mass m, and there are N of them in total. The rotation of the system is measured via the angle of r_0, which is referred to as θ_0.

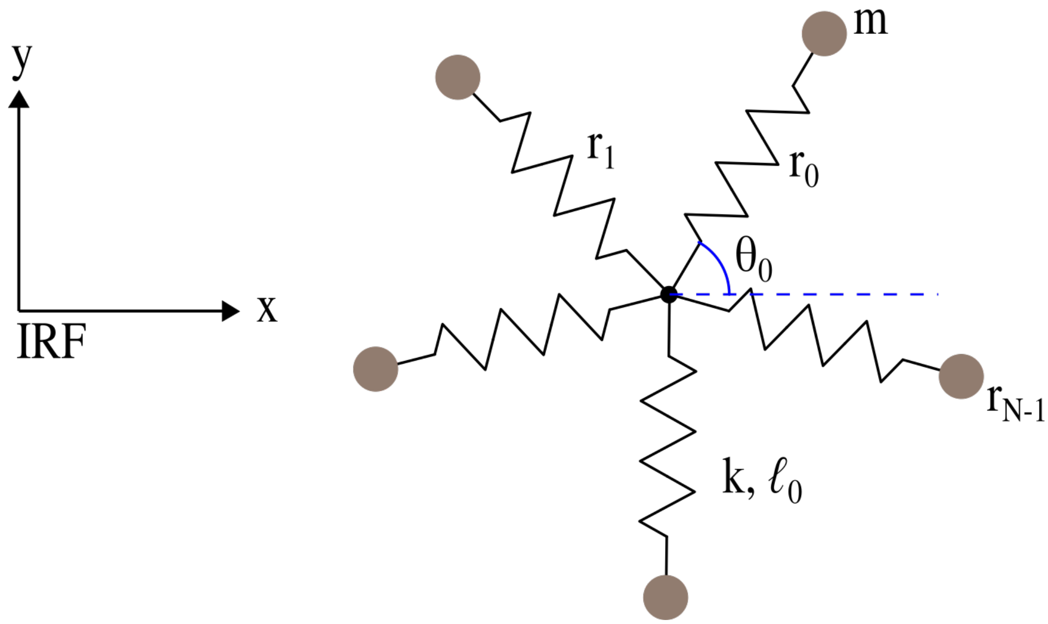

One important thing to note is that this model cannot enforce all radii to be the same. r_0, the radius of the first arm, might be different than r_1 due to gravitational effects. Keeping this in mind, we will first model the most general version of this system that we can, and then simplify as needed.

We begin by finding the coordinates and velocities of the involved objects:

$$\theta_n = \theta_0 + 2\pi \frac{n}{N} \tag{7}$$

$$\dot{\theta_n} = \dot{\theta_0} \equiv \omega \tag{8}$$

$$x_i = r_n \cos(\theta_n) \tag{9}$$

$$y_i = r_n \sin(\theta_n) \tag{10}$$

$$\dot{x_n} = \dot{r_n} \cos(\theta_n) - r_n \sin(\theta_n)\dot{\theta_0} \tag{11}$$

$$\dot{y_n} = \dot{r_n} \sin(\theta_n) + r_n \cos(\theta_n)\dot{\theta_0} \tag{12}$$

Now, we can model the kinetic energy of the system.

$$T = \sum_{n=0}^{N-1} \frac{1}{2} m(\dot{x_n}^2 + \dot{y_n}^2) \tag{13}$$

$$= \frac{m}{2} \sum_{n=0}^{N-1} (\dot{r_n} \cos(\theta_n) - r_n \sin(\theta_n)\dot{\theta}_0)^2 + (\dot{r_n} \sin(\theta_n) + r_n \cos(\theta_n)\dot{\theta}_0)^2 \tag{14}$$

$$= \frac{m}{2} \sum_{n=0}^{N-1} \left(\dot{r_n}^2 + r_n^2 \dot{\theta_0}^2 \right) \tag{15}$$

Next, we find the potential energy:

$$U = \sum_{n=0}^{N-1} \left(\frac{1}{2} k(\ell_0 - r_n)^2 + mgr_n \sin(\theta_n) \right) \tag{16}$$

Finally, we can combine these to yield the lagrangian for this system.

$$\mathscr{L} = T - U \tag{17}$$

$$= \sum_{n=0}^{N-1} \frac{m}{2} \left(\dot{r_n}^2 + r_n^2 \dot{\theta_0}^2 \right) - \frac{1}{2} k(\ell_0 - r_n)^2 - mgr_n \sin(\theta_n) \tag{18}$$

Now, we can find the Euler-Lagrange equations. This system has $s = N + 1$ degrees of freedom. N of these are given by the parameters $r_0, r_1, \ldots, r_{N-1}$, and the final parameter is θ_0.

Although we do technically have $N + 1$ Euler-Lagrange equations, N of them will be indistinguishable due to symmetry. We'll begin with the equation for the angle:

$$\frac{\mathrm{d}}{\mathrm{d}t} \left(\frac{\partial \mathscr{L}}{\partial \dot{\theta}_0} \right) = \frac{\mathrm{d}}{\mathrm{d}t} \sum_{n=0}^{N-1} m\dot{\theta}_0 r_n^2 \tag{19}$$

$$= m \sum_{n=0}^{N-1} \ddot{\theta}_0 r_n^2 + 2r_n \dot{\theta}_0 \dot{r_n} \tag{20}$$

$$= \frac{\partial \mathscr{L}}{\partial \theta_0} = -mg \sum_{n=0}^{N-1} r_n \cos(\theta_n)\dot{\theta}_0 \tag{21}$$

$$\tag{22}$$

Dividing out the common m term, we see that the equation simplifies to the following.

$$\sum_{n=0}^{N-1} \ddot{\theta_0} r_n^2 + 2 r_n \dot{\theta_0} \dot{r_n} = -g \sum_{n=0}^{N-1} r_n \cos(\theta_n) \dot{\theta_0} \tag{23}$$

We'll now compute the Euler-Lagrange equations for the remaining N parameters - however, as mentioned, the symmetry of the problem means this is really just a single computation.

$$\frac{\mathrm{d}}{\mathrm{d}t} \left(\frac{\partial \mathscr{L}}{\partial \dot{r_n}} \right) = \frac{\mathrm{d}}{\mathrm{d}t} (m \dot{r_n}) = m \ddot{r_n} \tag{24}$$

$$= \frac{\partial \mathscr{L}}{\partial r_n} = \left(m \dot{\theta_0}^2 r_n + k(\ell_0 - r_n) - mg \sin(\theta_n) \right) \tag{25}$$

Motivated by the math of a simple spring oscillation, we'll introduce the fundamental frequency, $\omega_0 = \sqrt{\frac{k}{m}}$, into this calculation by dividing mass through.

$$\ddot{r_n} = \dot{\theta_0}^2 r_n + \frac{k}{m}(\ell_0 - r_n) - g \sin(\theta_n) \tag{26}$$

$$= \dot{\theta_0}^2 r_n + \omega_0^2 (\ell_0 - r_n) - g \sin(\theta_n) \tag{27}$$

To summarize, our Euler-Lagrange equations are shown below.

$$\ddot{r_n} = \dot{\theta_0}^2 r_n + \omega_0^2 (\ell_0 - r_n) - g \sin(\theta_n), \ \forall n \in [0, N-1] \tag{28}$$

$$\sum_{n=0}^{N-1} \ddot{\theta_0} r_n^2 + 2 r_n \dot{\theta_0} \dot{r_n} = -g \sum_{n=0}^{N-1} r_n \cos(\theta_n) \dot{\theta_0} \tag{29}$$

4 Analysis

The equations that we just derived are a little too rich to solve by hand (for a third year, at least), but we can further simplify them to find some important truths.

For our analysis, we'll restrict N to being 1, and then use a small oscillation approximation to compute the system's properties. This may seem overly restrictive, but will provide some insight into how the changing spring angle affects its extension.

We begin by formulating our reduced lagrangian:

$$\mathscr{L}_r = \frac{m}{2}\left(\dot{r}^2 + r^2\dot{\theta}^2\right) - \frac{1}{2}k(\ell_0 - r)^2 - mgr\sin\theta \tag{30}$$

To use a small oscillations approximation, we'll first taylor expand around the global minimum of U, namely $(r, \theta) = (\ell_0, 0)$.

$$\mathscr{L}_r \approx \frac{m}{2}\left(\dot{r}^2 + \ell_0^2\dot{\theta}^2\right) - mgr\theta \tag{31}$$

This has allowed us to reduce overall nonlinearity, as well as remove the sinusoid. Next, we'll take the Euler-Lagrange equations:

$$\begin{aligned} \frac{\mathrm{d}}{\mathrm{d}t}\left(\frac{\partial\mathscr{L}}{\partial\dot{r}}\right) &= \frac{\mathrm{d}}{\mathrm{d}t}\left(m\dot{r}\right) = m\ddot{r} && (32)\\ &= \frac{\partial\mathscr{L}}{\partial r} = -mg\theta && (33)\\ \implies \ddot{r} &= -g\theta && (34)\\ & && (35) \end{aligned}$$

$$\begin{aligned} \frac{\mathrm{d}}{\mathrm{d}t}\left(\frac{\partial\mathscr{L}}{\partial\dot{\theta}}\right) &= m\ell_0^2\ddot{\theta} = \frac{\partial\mathscr{L}}{\partial\theta} = mgr && (36)\\ \implies \ell_0^2\ddot{\theta} &= gr && (37) \end{aligned}$$

Now, we'll employ the small oscillations approximation. Note that the constants are in different units - length (A) and angle (B).

$$\begin{aligned} r(t) &\equiv A\cos(\omega t + \phi) && (38)\\ \theta(t) &\equiv B\cos(\omega t + \phi) && (39) \end{aligned}$$

$$\ddot{r} = -\omega^2 A \cos(\omega t + \phi) \tag{40}$$
$$= -g\theta = -gB\cos(\omega t + \phi) \tag{41}$$
$$\implies \omega^2 A = gB \tag{42}$$
$$\tag{43}$$

$$\ell_0^2 \ddot{\theta} = \ell_0^2 B \omega^2 \cos(\omega t + \phi) \tag{44}$$
$$= gr = gA\cos(\omega t + \phi) \tag{45}$$
$$\implies \ell_0^2 \omega^2 B = gA \tag{46}$$

We cannot solve for all three of these new parameters with only two equations, so we'll solve simply for ω and the ratio of amplitudes, $C \equiv \frac{A}{B}$.

$$\omega^2 \frac{A}{B} = \omega^2 C = g \tag{47}$$
$$\implies C = \frac{g}{\omega^2} \tag{48}$$
$$\frac{\ell_0^2 \omega^2}{g} = C \tag{49}$$
$$\implies \frac{g}{\omega^2} = \frac{\ell_0^2 \omega^2}{g} \tag{50}$$
$$\implies g^2 = \ell_0^2 \omega^4 \tag{51}$$
$$\implies g = \pm \ell_0 \omega^2 \tag{52}$$
$$\implies \omega = \pm \sqrt{\frac{g}{\ell_0}} \tag{53}$$

Note that we ignored two of the ω solutions, because they were complex. This is an interesting conclusion, but should not be particularly surprising. When the spring oscillations are very small, the system behaves like a planar pendulum with classical frequency $\sqrt{\frac{g}{L}}$.

Next, we will find the ratio of amplitudes:

$$C = \frac{g}{\omega^2} = \ell_0 \tag{54}$$

Phrased more clearly, this means that $A = \ell_0 B$ - the spring oscillates with the amplitude of the pendulum's angle, multiplied by the rest length. Importantly, this also means that the spring oscillation is particularly sensitive to the centrifugal action.

5 Numerical Approximation

In the previous sections, we examined this system from an analytical perspective. However, finding exact solutions of the motion of this system is likely not possible (as is true of many systems). To better understand the behavior of a variable-radius reaction wheel, we'll turn to numerical simulations.

First, we must convert our euler-lagrange equations into a finite difference approximation. The r equations were transformed using the central difference approximation of $\ddot{r}_i$, and the backward difference approximation of $\dot{\theta}_0$. The angular equation used a forwards difference approximation of $\dot{theta}$. These choices seem arbitrary, but allow the r_n term to be more easily solved for. Additional documents showing these transformations are available in this project's github repository